Article

Not peer-reviewed version

Raman Technology for Process Control: Waste Shells Demineralization to Produce Transparent Polymer Foils Reinforced with Natural Antioxidant, and Calcium Acetate By-Product

Simona Cinta Pinzaru *, Iuliana-Cornelia Poplăcean *, Karlo Maškarić, Danut-Alexandru Dumitru, Lucian Barbu-Tudoran, Tudor Liviu TĂMAȘ, Fran Nekvapil, Bogdan Neculai

Posted Date: 15 March 2024

doi: 10.20944/preprints202403.0918.v1

Keywords: Raman technology; recovery and resource utilization technology; process control; biogenic carbonate waste; chitin; calcium acetate drug; carotenoids.

Article

Raman Technology for Process Control: Waste Shells Demineralization to Produce Transparent Polymer Foils Reinforced with Natural Antioxidant, and Calcium Acetate By-Product

Simona Cînta Pînzaru [1,2,*], Iuliana-Cornelia Poplăcean [1,*], Karlo Maškarić [1,2,*], Dănuț-Dumitru Alexandru [1], Lucian Barbu-Tudoran [3,4], Tudor Tămaș [5], Fran Nekvapil [1,2,3] and Neculai Bogdan [6]

[1] Babeş–Bolyai University, Biomolecular Physics Department, Kogălniceanu 1, 400084, Cluj-Napoca, Romania; simona.pinzaru@ubbcluj.ro
[2] Institute for Research, Development and Innovation in Applied Natural Sciences, Babeș-Bolyai University, Fântânele 30, Cluj-Napoca, Romania; lucian.baia@phys.ubbcluj.ro
[3] National Institute for Research and Development of Isotopic and Molecular Technologies, Donath 67-103, 400293 Cluj-Napoca, Romania; itim@itim-cj.ro
[4] Electron Microscopy Center, Babeș-Bolyai University, Clinicilor 5-7, 400006 Cluj-Napoca, Romania; e-mail: lucianbarbu@yahoo.com
[5] Department of Geology, Babeș-Bolyai University, M. Kogălniceanu 1, 400084 Cluj-Napoca, Romania; tudor.tamas@ubbcluj.ro
[6] Metrohm Analytics Romania SRL, E. Racoviţă 5, 041753 Bucharest, Romania; bogdan.neculai@metrohm.ro
* Correspondence: simona.pinzaru@ubbcluj.ro; iuliana.poplacean@stud.ubbcluj.ro, karlo.maskaric@ubbcluj.ro

Abstract: Waste biogenic materials from seafood exploitation are valuable resources of new compounds exploitation within the blue bioeconomy concept. Here, we describe the effectiveness of Raman technology implementation as an in-line tool for demineralization process control of crustaceans or gastropods. We produced transparent chitin polymer foils from three waste crustacean shells (*C. sapidus, S. mantis and M. squinado*) using a slow, green chemical approach employing acetic acid, and showed the progressive process of biogenic carbonate dissolution and increasing the Raman characteristic signal of chitin, in a time dependence manner. It turned that chitin foils obtaining is species-specific, and the demineralization bath of waste shell mixture can be effectively tracked by Raman spectroscopy, for solvent control and the recovery of the calcium acetate as valuable by-product. Comparatively, calcium acetate drug, a compound widely used in kidney failure diseases, or as additive in nutraceuticals and food industry, has been obtained here, following a green demineralization path of the sea snail *Rapana venosa* intact shell, assisted by Raman technology, using 9% acetic acid (vinegar) solution for 14 days. To validate the final products identity and quality, The process of waste shells demineralization and the final products of the treatment were investigated using various Raman techniques and technologies, cross-validating the results with FT-IR, XRD and SEM-EDX techniques. NIR Raman spectroscopy revealed chitin bands in a time-dependent manner, while Resonance Raman spectroscopy showed the preservation of carotenoids after two weeks of acetic acid treatment. A hand-held flexible TacticID Raman system with a 1064 nm excitation demonstrated its effectiveness as a rapid, in-line decision making tool during process control and revealed excellent reproducibility of the lab-based instrument signal, suitable for in situ evaluation of the demineralization status and solvent saturation control. The calcium acetate recovered from residual treatment solutions was assessed regarding its hydration status, purity, and suitability as recrystallized material for further use as pharmaceutical product or ingredient in complex formulations.

 doi:10.20944/preprints202403.0918.v1

Keywords: Raman technology; recovery and resource utilization technology; process control; biogenic carbonate waste; demineralization process control; chitin; calcium acetate drug; carotenoids

1. Introduction

The demineralization of crustacean shells has wide applicability not only in materials science but also in aquatic research and environmental studies, as well as in the currently increasing demand of the bioeconomy sector. The main objective of the blue bioeconomy is to obtain new and valuable products from aquatic waste, making it one of the rapidly expanding research fields in the context of current priorities [1].

The abundant aquatic waste material in focus here is the biogenic calcium carbonate originating from crustacean or gastropod shells. Among these, the Atlantic blue crab *Callinectes sapidus* (Rathbun, 1896) and whelk *Rapana venosa* (Valenciennes, 1846) are ranked as some of the most invasive species in the Mediterranean and Black Sea basins. There are many studies related to the increased awareness regarding the most invasive species in the Mediterranean Sea such as the one conducted by Marchessaux et al. who advocate the resilient idea of turning the threat into new opportunities [2–4].

The Atlantic blue crab *C. sapidus* and the whelk *R. venosa* are both ranked among the 100 worst invasive species, with a negative impact on the ecology of invaded areas, seashore ecosystems, touristic areas, as well as the aquaculture exploitation of the local bivalve products. These species have raised special attention not only from environmental scientists, but also from the blue bioeconomy research field due to their potential for multidisciplinary approaches. Thus, aquatic resources can be sustainably exploited to produce value-added compounds or innovative products from aquatic waste.

We demonstrated in several recently published papers that the highly ordered 3D-nanostructure of the *C. sapidus* shells, comprising mineral and organic components [5], possesses an intricate porosity, which could be exploited for various applications [6]. These include serving as an efficient material for solutions loading and slow release [7,8], a drug carrier, or an efficient absorbent of pollutants [9], as well as a new biostimulant [10], while being compliant with the regulations regarding their heavy metal content [11].

The complex scaffold of chitin-protein fibrils that supports biomineralization has never been considered with respect to its potential utility as a chitin–based polymer foil. This green product might be available as a subject of the intact raw material demineralized, without powdering. As recently reviewed, numerous studies reporting chitin or chitosan production from crustaceans [12] have used powdering as a main step in the production process, where understanding dependencies for efficient extraction is crucial. To speed up the process, the energy consumption and the workload for the multi-step preparation of powders are high, while a slower process could eliminate all these steps. The demineralization process, however, can be considered without powdering, heating, and stirring of the demineralization bath, conducting to a resulted material that can be further tailored according to the desired products.

Chitin, the second most abundant polymer after cellulose, is widely produced from the primary source of aquatic waste derived from crab and shrimp processing waste bioeconomy. Industrially, chitin is produced throughout acid treatment, hydrochloric acid being the preferred demineralization agent, even though it may negatively impact the molecular mass and the degree of deacetylation of the resulted polymer. Therefore, it may impair the purified chitin's inherent qualities [13]. The demineralization process is followed by deproteinization and decolorization to obtain pure, colorless chitin, without any residues, reaching the required quality for specific applications of many fields, such as drug delivery, tissue engineering, agriculture, food industry and others [12]. Due to the variability of the chitin source, the entire production process requires optimization.

To obtain chitin from various crustacean species, the demineralization process may depend on the structural and morphological characteristics of each species, thus knowledge-based decisions on

 doi:10.20944/preprints202403.0918.v1

the most convenient process steps are required. Additionally, during the demineralization process, tools needed for informed decisions (to continue, to modify conditions or to stop) are scant. Most of the studies rely on obtaining the "final product" under certain conditions and consider the necessary repeating operations or improved conditions to achieve the optimal processing. This is done with the aim of ensuring compatibility with the transition to the industrial environment to the highest technology readiness level (TRL), while complying with low cost, high-quality final product, minimal workload and an environmentally friendly chemical consumption [14].

When exposed to acid treatment (usually hydrochloric acid), the biogenic carbonate reacts to yield the secondary product, calcium acetate, besides CO_2 and water. Calcium acetate, approved by the regulatory bodies [15], is widely used as a food additive, an acidity regulator, a preservative and stabilizing agent for nutraceuticals, a calcium supplement, and as a medication for patients with kidney disease undergoing dialysis, to control hyperphosphatemia. There are two widely used industrial methods to obtain calcium acetate. One involves the reaction between calcium carbonate and acetic acid, often using natural limestones or marble as the starting material, resulting calcium acetate, carbon dioxide, and water. The other method employs using calcium hydroxide and acetic acid, yielding calcium acetate and water. The biogenic carbonate waste material, typically referring to calcium carbonate derived from the crustaceans' waste, bivalve, or molluscs shells, is not usually considered, as it is often blamed for potential impurity residues that may alter the quality of the calcium acetate product.

To the best of our knowledge, there are neither reported studies on obtaining transparent polymeric foils of chitin from unground, unpowdered biogenic materials derived from *C. sapidus*, the mantis shrimp *Squilla mantis* (Linnaeus, 1758), and the European spider crab *Maja squinado* (Herbst, 1788), nor reports on calcium acetate obtained from these crustaceans. Md. Iftekhar Shams et al. noted the preparation of an optically transparent crab-shell by removing non-chitin components (e.g. calcium carbonate, proteins, lipids, pigments) to create transparent nanocomposites with improved properties. The species considered was *Chionoecetes opilio* (Fabricius, 1788), and the demineralization process occurred under hydrochloric acid treatment [16].

In this paper we demonstrate the usefulness of the Raman spectroscopy techniques to assist the demineralization process of the biogenic carbonates derived from three distinct crustacean species to obtain chitin, or derived from *R. venosa* shells, to valorize its abundant calcium content for calcium acetate production, as this gastropod shell does not comprise chitin. We compared the in-line process control results in terms of Raman spectroscopy signal, to timely check the appearance of the chitin signal in the resulting demineralized biological samples using both the lab-based Raman system and the hand-held Raman instrument. We further comparatively evaluate the calcium acetate by-products resulted after applying a 'green' method, using the acetic acid reaction on the biogenic waste at room temperature, without powdering or heating. Finally, we evaluate the quality of the calcium acetate resulted from the crustaceans and snail shells. Fourier-transform infrared spectroscopy (FT-IR), X-ray diffraction (XRD) and scanning electron microscopy combined with energy dispersive X-ray spectroscopy (SEM-EDX) have been employed as cross validation methods to confirm the identity and the morphology of the final bio-products.

Considering the time, cost, effort and chemicals required for such a crucial industrial approach, here we propose the implementation of Raman technology as an effective tool to assist every step of this economically important activity.

2. Materials and Methods

2.1. Biogenic Material Selection and Processing

Biological samples from three crustacean species – *C. sapidus, S. mantis and M. squinado* - were acquired through a collaboration between the Babeș-Bolyai University and the University of Dubrovnik, originating from the Neretva River Delta (South-Easten Adriatic Sea). The specimens of *S. mantis* and *M. squinado* were caught and maintained in frozen conditions, while the shells from *C. sapidus* represented food waste from cooked crabs. One specimen from each *S. mantis* and *M. squinado*

 doi:10.20944/preprints202403.0918.v1

were eviscerated. We considered waste biogenic material from cooked carapace fragments of *C. sapidus*, cuticle segments of abdomen, telson cuticle from *S. mantis* and the whole, raw carapace of *M. squinado* for the experimental studies. Fresh specimens of the *R. venosa* snail have been gathered from a cluster of individuals along the Romanian shores of the Black Sea, specifically Năvodari, at the geographical coordinates 44°18'07.4"N, 28°37'38.4"E. The *R. venosa* shells were randomly selected from a large stock comprising both adult specimens with intensive pink-orange pigmentation and juvenile specimens with pronounced blue pigmentation.

The selected crustacean shells were cleaned from adherent aquatic materials, degreased, washed abundantly with deionized pure water (resistivity 18.2 MΩ × cm at 22°C) and immersed in pure glacial acetic acid. *R. venosa* specimens were immersed in a vinegar bath (acetic acid 9%), after undergoing a thorough cleaning process with the removal of soft tissue from the shells. Demineralization occurred at room temperature, with the process systematically monitored through periodic analysis of the biological samples by Raman techniques.

2.2. Chemicals

Glacial acetic acid was provided by Sigma Aldrich, while geogenic calcium carbonate was purchased from CHIMREACTIV S.R.L, both substances being used without any further purification.

2.3. Demineralization By-Products and Reference Calcium Acetate Synthesis

The immersion bathing solutions of the biological samples were evaporated by exposure to controlled heat to fully investigate the demineralization process. Given that calcium carbonate is the main mineral of the biological samples considered, the reaction between this compound and acetic acid was observed to obtain geogenic calcium acetate as a reference material of the demineralization by-products. Geogenic calcium acetate was synthetized using 1 mg of standard geogenic calcium carbonate dissolved in a mixture solution of 2 ml pure glacial acetic acid and 3 ml acetic acid aqueous solution 10%. The obtained mixture was prepared under magnetic stirring at controlled temperature for 60 minutes, the resulted solution being evaporated under controlled heat. All powders obtained were dried in the oven at 60°C for 24 hours and investigated through Raman spectroscopy and X-ay diffraction.

2.4. Instrumentation

As a lab-based instrument to validate the hand-held Raman system, we employed the Renishaw InVia Reflex Raman system (Renishaw, UK) with a Leica confocal microscope. For Raman excitation, a laser diode emitting at 785 nm has been employed to characterize the starting materials and the ones during the demineralization progress. An additional Cobolt diode pumped solid state laser emitting at 532 nm has been employed to control the presence of native carotenoids in biogenic shells, exploiting their selective signal under resonance Raman conditions, and a He-Ne- laser providing the 632.8 nm excitation line has been used for detecting the carotenoproteins resonant signal. The instrument calibration was achieved with the internal silicon providing the band centred at 520 cm^{-1}. WiRE™ 3.4 Software (Renishaw, United Kingdom) was used for data acquisition. The spectral resolution was 1 cm^{-1} in NIR and 0.5 cm^{-1} for the visible range excitation.

A hand-held TacticID® Mobile Raman system model BWS493TSII (BWTEK, a Metrohm Group Company) with a NIR-laser emitting at 1064 nm, 220 mW with a TE-Cooled InGaAs Array detector, has been used to record spectra during process in the 176 - 2000 cm^{-1} spectral range, with a spectral resolution of 11 cm^{-1}. The system is equipped with a database of 1200 spectra of synthetic chemicals, narcotics, drugs, explosives, cutting agents, precursors, and solvents [17].

A Shimadzu FT-IR IRSPIRIT with an QATR-S accessory, holding a single-reflection integration-type ATR module, with a diamond prism, has been employed to record the FT-IR spectra of the demineralized fragments in the 650-4000 cm^{-1} spectral range, setting 50 accumulations per spectrum, with 8 cm^{-1} spectral resolution selected in the LabSolutions IR software.

 doi:10.20944/preprints202403.0918.v1

X-ray powder diffraction (XRD) analyses were achieved using a Bruker D8 Advance diffractometer in Bragg-Brentano geometry, possessing a Cu tube with λ_{K_α} = 0.15418 nm, a Ni filter and a LynxEye detector. Corundum (NIST SRM1976a) was used as an internal standard. The data were collected in the 3.8 – 64° 2θ interval at a 0.02° 2θ step, measuring each step for 0.2 seconds. Acetate precipitates were ground in an agate mortar and placed in Bruker PMMA sample holders. In the case of the demineralized foils, surface XRD was performed on foil fragments, with the surface of the fragments aligned to the X-ray beam. The identification of mineral phases was performed with the Diffrac.Eva 2.1 software (Bruker AXS) using the PDF2 (2023) database from the ICDD (International Centre for Diffraction Data).

Scanning electron microscopy and energy-dispersive X-ray spectroscopy (SEM-EDX) analyses have been achieved using a Hitachi SU8320 ultra-high resolution cold field emission scanning electron microscope (Hitachi, Japan) with a Quorum Q150T gold sputtering coater of controlled thickness of 11 nm at a rate of 14 nm/min and evaporating carbon for EDX analysis using an Oxford energy-dispersive X-ray module (Oxford, UK) for semiquantitative elemental analysis of the demineralized shell fragments.

The dataset underwent comprehensive processing and analysing using OriginPro 2021b, OriginLab Corporation, Northampton, MA, USA. The data processing steps are illustrated in the supplementary figure (Figure S1) which includes recording multiple spectra, calculating averaged signal, background subtraction, and comparison with the reference spectral data of α-chitin.

3. Results and Discussion

3.1. Demineralization Process

Stock of selected materials for exploring the green demineralization process, consisting of untreated fragments of crustacean shells, are shown in Figure 1A. All the anatomical fragments were subjected to the same demineralization treatment, described above. Following the applied treatment, transparent and flexible samples were obtained, as noted in Figure 1B. Besides, the disappearance of the stiffness indicates the dissolution of the mineral component of the crustaceans' shells (Video S1). The process was accompanied by the extraction of carotenoids, leading to the discovery of acetic acid's role in the depigmentation of crustacean shells. In the case of *R. venosa*, Figure 1C highlights the effects of shell demineralization after 14 days of vinegar immersion. The fully developed specimen showed overall different prominent signs of shell degradation from the appearance of through holes, shell apex withdrawal, and strong interior depigmentation. Furthermore, fragments of the exterior side shell layer with brown pigmented lines started to detach from the still-solid body.

 doi:10.20944/preprints202403.0918.v1

Figure 1. (A) Untreated anatomical parts as following: carapace fragments (a) and ventral fragment (b) of *C. sapidus*; cuticle segments of abdomen (c), uropod (d) and telson cuticle (e) from *S. mantis*; carapace of *M. squinado* (f); (B) Crustacean anatomical shell fragments after exposure to acetic acid for 65 days as following: carapace fragment (a) and ventral fragment (b) of *C. sapidus*; cuticle segment of abdomen (c), uropod (d) and telson cuticle (e) from *S. mantis*; carapace of *M. squinado* (f); (C) Adult *R. venosa* shell during vinegar demineralization (a) and after 14 days of treatment in ventral (b) and lateral (c) view.

3.2. Raman Spectral Analyses during the Demineralization Process

The Raman spectra of the starting materials were checked to comply with the already known characteristics: under 785 nm excitation, the crab species shells exhibit the dominant, characteristic bands of calcite at 1085, 712, 281 and 156 cm^{-1}, weak bands of pigments (free and non-covalently bond astaxanthin showing the C=C stretching modes at 1516 and 1494 cm^{-1} respectively) and several weak trace of bands originating from the most intense modes of chitin above a typical background, even for NIR excitation. Particularly, in case of *S. mantis* shell, besides the above bands typical for crabs, a strong band is observed from phosphate at 954 cm^{-1}, which is overlapped with the more prominent chitin bands. To track the demineralization process under acetic acid exposure, we have analysed the biological samples at different moments of time, marked in Figure 2 for each individual crustacean specimen.

By monitoring the evolution of the Raman spectrum of the crustacean shells, from typically raw biogenic calcium carbonate presence to the appearance of the characteristic signal of chitin and the disappearance of the calcium carbonate Raman bands at 1085, 712, 281 and 156 cm^{-1}, the spectra taken during the process control promptly guided decision-making regarding whether to stop or to continue the acetic acid exposure of the crustacean shells. It turned out that the different species required varying durations for complete demineralization, the thick carapace of *M. squinado* requiring a longer exposure compared to the shell fragments of *C. sapidus* or *S. mantis*.

The Raman spectra of the biogenic material from *C. sapidus* after acetic acid exposure are shown in Figure 2A. The presence of calcium carbonate in the polymorphic form of calcite is revealed by the Raman spectra acquired from the *C. sapidus* untreated shell and the one exposed to acetic acid for 20

 doi:10.20944/preprints202403.0918.v1

hours. Additionally, the strongest band in the astaxanthin Raman spectrum is also present in the spectra of the two discussed samples. The α-chitin specific signals start to appear only after exposure to acetic acid, being covered by the background in the case of the untreated fragment shell. After 140 hours of immersion in acetic acid, the *C. sapidus* shell fragment has been completely demineralized. Thus, through exposure to acetic acid, markedly weaker acid than the hydrochloric acid which is commonly employed in many previous studies [12], the process of dissolving the mineral component in crustacean shells yielded promising outcomes. Following this success, we have monitored the evolution of the chitin Raman bands through an extended acetic acid treatment. Once the exposure time increased, the Raman spectrum acquired on the shell fragments began to show an improved spectral resolution of the α-chitin signal. After 65 days of immersion in acetic acid, the spectrum of the shell fragment from the *C. sapidus* presented the bands of the reference α-chitin with highest accuracy. Additional vibrational bands express the presence of lipids and proteins in fragments of *C. sapidus* shells exposed to acetic acid.

The different time needed for chitin clear bands appearance along the demineralization process could be explained by the fact that the various parts of the crab shell have different composition and thickness [18]. Talking about our biological samples, the whole carapace of *M. squinado* is more mineralized and thicker than the S. mantis cuticles, thus, the latter experienced faster demineralization and clear observation of chitin Raman bands occurrence. The earliest chitin bands were observed after 18 hours of acetic acid bath treatment (Figure 2B). Calcium carbonate Raman signal was still present after two weeks of treatment in the carapace of *M. squinado*, indicating an intricate structure and low demineralization process (Figure 2C).

Time-dependent Raman spectra acquired under 785 nm excitation revealed different chitin bands in the case of *S. mantis* and *M. squinado*. The first chitin bands observed after 18 hours treatment in *S. mantis* are present at other points in time. In the case of *M. squinado*, the first chitin bands were visible two weeks after the treatment. At the same time, calcium carbonate bands at 152 cm^{-1}, 281 cm^{-1}, 1087 cm^{-1} were still present. Besides chitin and calcium carbonate, the peaks with the highest intensity are those from the carotenoids and the carotenoproteins (Figure 3). The excitation of the carapace at the end of the treatment (after 65 days) revealed a high background from the remaining proteins (Figure 2C). Due to the high background, calcium carbonate bands might not be seen. Carotenoids seem not to be present at the time, or the point of the carapace did not contain carotenoids. The colour originating from carotenoids is still visible with the naked eye at the end of the treatment (Figure 1B).

 doi:10.20944/preprints202403.0918.v1

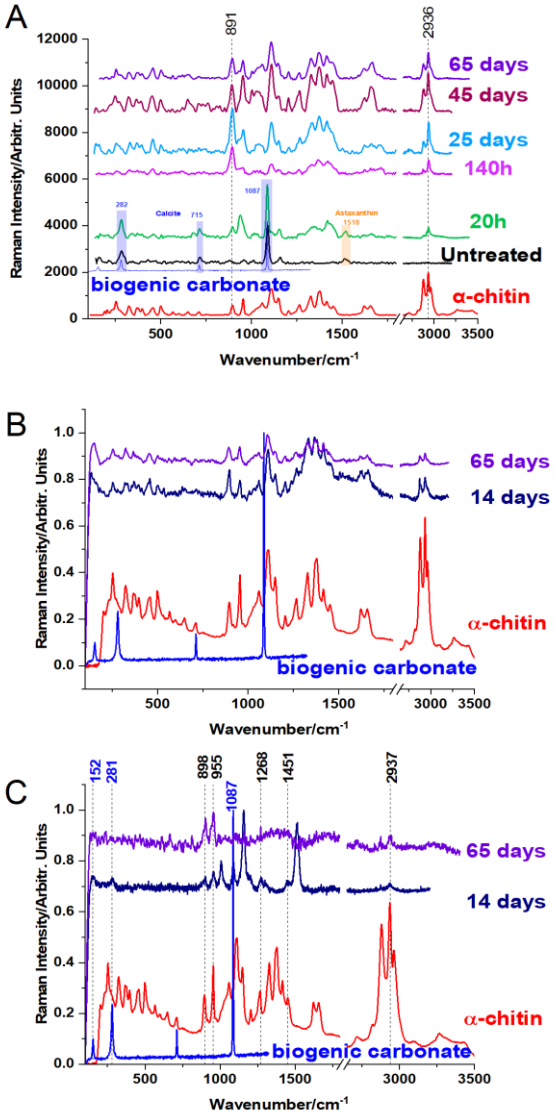

Figure 2. Raman spectra evolution of the biogenic material from *C. Sapidus* (A), *S. mantis* (B), and *M. squinado* (C) at various times (indicated as hours or days) during the acetic acid demineralization process, using 785 nm laser line, compared to the reference spectrum of α-chitin, as indicated. The blue spectra show the reference signal of calcium carbonate to highlight its disappearance in the final products.

The crab cuticles contain carotenoids and carotenoproteins as Figure 3 shows. The carotenoids were still present after 14 days of acetic acid bath solution. In the case of *C. sapidus* and *M. squinado*, the carotenoids profile did not experience shifts in the wavenumber position but appeared with lower relative intensity (Figure 3A, C). *S. mantis* carotenoids exhibited shifts in the wavenumber position and the relative intensities of the vibrational bands got lower after acetic acid treatment (Figure 3B).

Preprints.org (www.preprints.org) | NOT PEER-REVIEWED | Posted: 15 March 2024 doi:10.20944/preprints202403.0918.v1

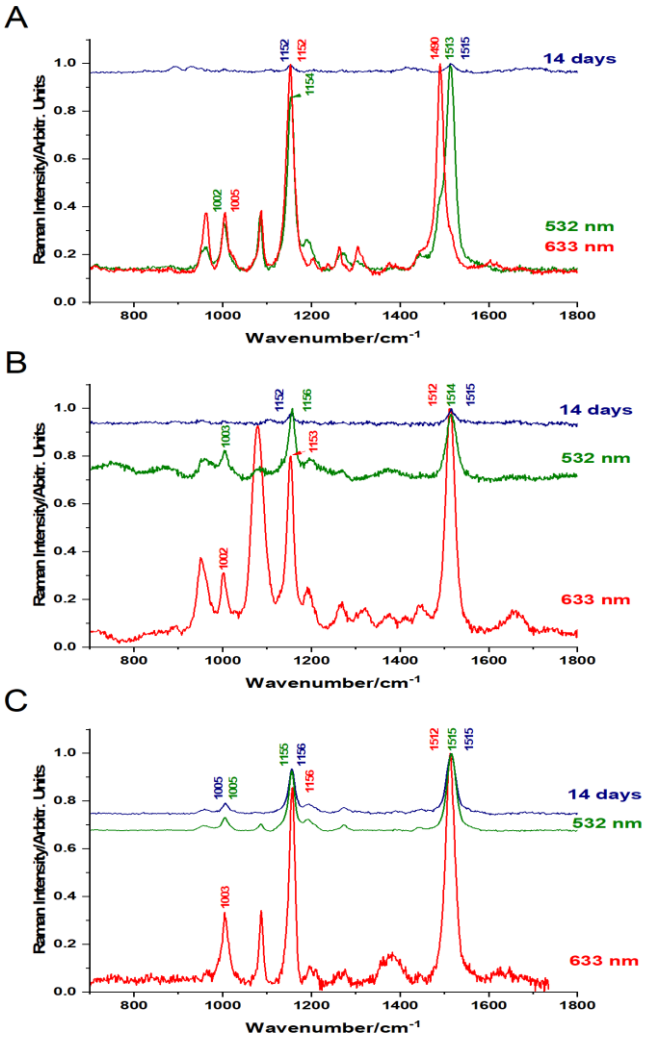

Figure 3. Pigments detected in the raw crustacean shells of *C. sapidus* (A), *S. mantis* (B), and *M. squinado* (C), under resonant Raman excitation with 532 nm for carotenoids (green line) and 633 nm for carotenoproteins (red line) before demineralization, and after 14 days of exposure to the acetic acid bath solution (top spectra, navy - blue line in each case).

3.3. Validation Results Using FT-IR Spectral Analyses of Demineralized Foil Products Derived from Crustaceans

The FT-IR spectra of the demineralized crustacean foils are shown in Figure 4. In case of all three crustacean species (*C. sapidus*, *S. mantis*, and *M. squinado*), some new vibrational bands were identified at the end of the demineralization process (65 days), besides specific vibrational signals previously reported for raw crustacean fragments [9]. Among these, chitin-specific FT-IR signals have been identified in all specimen fragments as following: 891 cm^{-1} (ring stretching), 1411 cm^{-1} (CH_2 bending and CH_3 deformation), 1628 cm^{-1} (stretching of amide I). *S. mantis* and *M. squinado* demineralized shell fragments also reveals chitin bands at 1113 cm^{-1} (asymmetric in phase ring stretching) and 1377 cm^{-1}, while the CO-stretching vibration was identified in the case of *C. sapidus* treated shell fragment at 1022 cm^{-1} [19,20].

 doi:10.20944/preprints202403.0918.v1

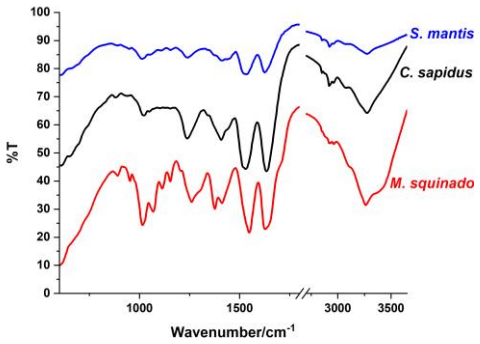

Figure 4. FT-IR spectra of the intact, transparent, demineralized foil products resulted from the three crustacean species after 65 days of acetic acid treatment: *S. mantis* (blue line), *C. sapidus* (black line), and M. *squinado* (red line).

3.4. Validation of the Demineralized Intact Foils Product Content Using X-ray Diffraction

The X-ray diffraction patterns of the demineralized foils from each of the three studied crustacean species are shown in Figure 5 . The presence of the characteristic peaks corresponding to the poly-glucosamine functional group, which are indicative of the structural framework of the chitin biopolymer, confirmed the demineralized foils' chitin content. The diffraction peaks were recorded around the following 2θ values: 9.2°, 19.3 °, 23.4 ° and 39°. These findings suggest that all three biological demineralized specimen fragments exhibit the same chitin semi-crystalline structure, consistent with previously reported characteristics of chitin extracted from insects and cuttlebone [21].

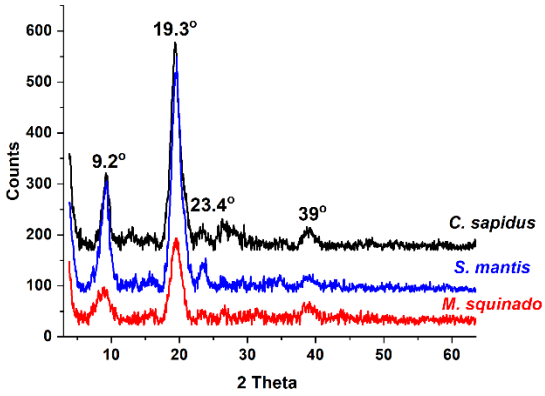

Figure 5. XRD diffraction patterns of the intact, transparent, demineralized foil products resulted from the three crustacean species after 65 days of acetic acid treatment: *C. sapidus* (black line), *S. mantis* (blue line), *M. squinado* (red line).

3.5. Validation of the Calcium Acetate By-Product Using X-ray Diffraction Patterns of the Crystallized Mineral from Acetate Bath Solutions

Aside from the production of demineralized biological shells, acetic acid treatment of the crustaceans' cuticle, and vinegar treatment of the gastropod led to calcium acetate production, a chemical of high interest in the medical field.

According to the XRD data of the calcium acetate resulted from the evaporated demineralization bathing liquid of the crustacean shells, the saturated solution indicates the resulted mixture of at least three distinct compounds: calcium acetate monohydrate, calcium acetate hemihydrate (calcium acetate half-hydrate) [22], and two additional peaks at 9.42° and 9.74° (Figure 6) which can be possibly assigned to calcium magnesium acetate hydrate as previously noticed [23].

 doi:10.20944/preprints202403.0918.v1

The calcium acetate produced from the blue crab (*C. sapidus*) is in fact a mixture of calcium hydrogen acetate (CaHAc 1:1:3) and calcium acetate monohydrate, while the geogenic form described above, and produced as reference, is composed of the half-hydrate form ($(CH_3COO)_2Ca \cdot 0{,}5\ H_2O$), as the X-ray diffraction patterns show. This form was the only one resulted from the demineralization solutions of the *R. venosa* specimens, both the pink and blue-pigmented shells. From these data we can conclude that using *R. venosa* shell waste for calcium acetate production might be more effective and this may be explained by the lower magnesium content of the *R. venosa* mineral shell (aragonite + calcite). In the case of the crustacean shells, the chitin flexible foils resulted from whole cuticle macro fragments as a compact polymer could be recovered preserving their shape integrity, while the organic component of the demineralized *R. venosa* shells, where chitin is not present, has been dispersed in the acetic acid solution once the biomineral part was dissolved.

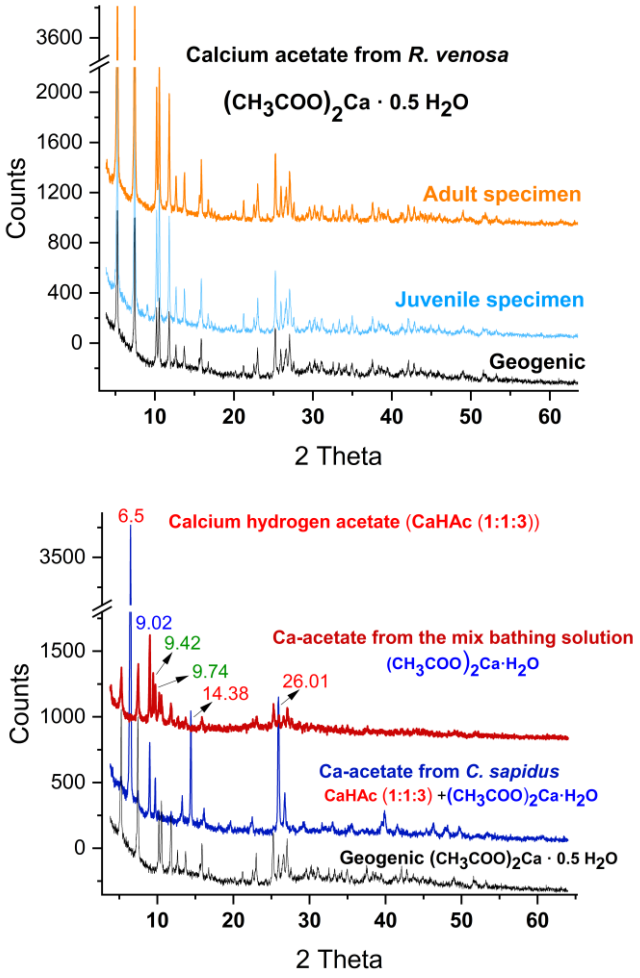

Figure 6. XRD pattern of the calcium acetate hemihydrate by-products from *R. venosa* snail (top panel): from adult pink shells (orange line), and juvenile blue pigmented shells (light-blue line). Calcium acetate by-products from crustaceans (bottom panel) shows different hydrated forms Ca-acetate from bathing solution of mixed crustacean shells (dark-red line), Ca-acetate from *C. sapidus* as a mixture of Ca-hydrogen acetate and hydrate (navy-blue line), and geogenic Ca-acetate hemihydrate (black line), as indicated on each pattern. Additional peaks in the Ca-acetate from bathing solution of mixed crustacean shells (dark-red line) plotted in green indicate other contributions.

3.6. Validation of the Calcium Acetate by-Product Using FT-IR of the Crystallized Mineral from Acetate Bath Solutions

To comprehend the structural variations between the obtained calcium acetate hydrates, Raman spectroscopic analyses of the powdered Ca-acetate by-products were conducted in addition to X-ray

 doi:10.20944/preprints202403.0918.v1

diffraction. When compared to the geogenic calcium acetate, all hydrates forms obtained as by-products of the demineralization process express slight structural changes marked by the shifting of specific vibrational bands, as shown in Figure 7. In the case of calcium acetate obtained from *R. venosa*, both the form resulted from the demineralization of an adult specimen and the one resulted from demineralization of a juvenile specimen exhibit a bands profile very similar to the geogenic compound. Despite the specific vibrational band of $\nu_s(CH_3)$ being shifted at 2927 cm^{-1}, a new vibrational signal appears at 664 cm^{-1} [24]. It can be attributed to an impurity. Regarding the calcium acetate forms obtained from crustaceans, both mix and only *C. sapidus*, the Raman spectra show the presence of specific vibrational bands of the geogenic form, but their profile is slightly different. Notable differences are observed in the case of *C. sapidus* calcium acetate by the new vibrational bands at 1693 cm^{-1} and 903 cm^{-1}, and the shift of the 1467 cm^{-1} signal. These marked differences can be attributed to the saturation of the bathing acetic acid liquid, as the XRD analyses also revealed through the identification of the calcium hydrogen acetate.

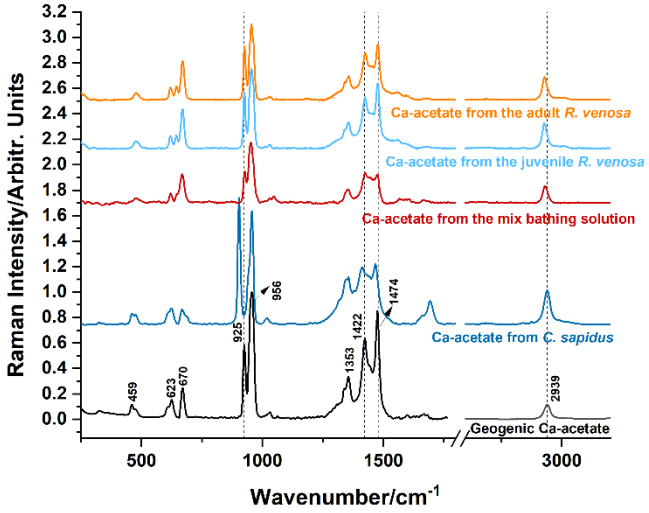

Figure 7. Calcium acetate hydrates formed in the demineralization bath solutions of adult (orange line) and juvenile *R. venosa* (light-blue line) specimens, mixed crustacean specimens (dark-red line), and *C. sapidus* (navy-blue line), compared to the geogenic calcium acetate (black line).

3.7. Demineralization Process Tracked with a Handheld TacticID Raman System

Using the hand-held Raman instrument, we were able to record the signal of the acetic acid bath solution comprising intact crustacean's cuticle fragments exposed to the demineralization process, as well as the minerals in various stages of demineralization. Additionally, three isolated and crystalized calcium acetate by-products could be tracked through the recipient or plastic bag sample. The advantage of the system relies on the possibility to accurately record the Raman spectrum of the bathing solution through the glass container. Thus, it is effective for controlling the bathing solution in terms of reagent consumption, the occurrence of the dissolved compounds during reaction, and the status of the intact fragments regarding their calcium carbonate dissolution, as illustrated in the Figure 8A. Along the process, the TacticID Raman instrument was used for detection of the chitin bands in the treated C. sapidus shell fragment after one week of the acetic acid treatment Figure 8B. The occurrence of the chitin bands in comparison with the reference α-chitin show linear correlation (R2= 0.998 and Pearson's r= 0.998), putting in value the employment of the system for optimizing the demineralization process Figure 8C.

 doi:10.20944/preprints202403.0918.v1

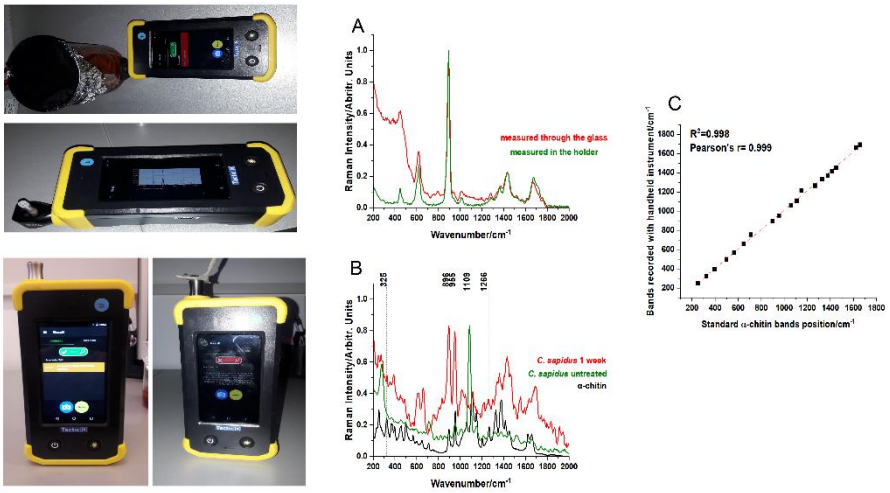

Figure 8. Using a hand-held TacticID Raman handheld instrument to control the demineralization process: images of the instrument at work and the displayed Raman spectra of the acetic acid bath solution (A); measured through the demineralization glass container (upper image, red line in the graph) and through its holder accessory for liquids (lower image, green line in the graph). (B) Setup of measurement of *C. sapidus* fragments: untreated (left image, green line in the graph) showing the strong calcium carbonate signal of raw shells and their disappearance after acetic acid treatment (right image, red line in the graph). The chitin reference signal is shown for comparison. Excitation: 1064 nm. (C) Linear correlation (R2= 0.998, Pearson's r=0.998) of the chitin bands recorded with TacticID Raman handheld instrument from the final foil product, with the standard α-chitin bands recorded with a lab-based instrument.

Compared to the lab-based Raman system, where, excitation with 785 nm of the demineralized shells in various stages results in highly fluorescence background, with several steps needed to process multiple data (please see Supplementary Figure S1), the hand held system incorporated technology for instantly "see" the processed signal without additional work-loading. The observed Raman bands collected from the resulted intact demineralized shells fragments of the three crustacean species are summarized in the Table 1. Besides the chitin bands, clearly observed either with the lab based or with the portable handheld instrument, several additional bands have been observed as shown in the Table 1. Those bands might be attributed to proteins or lipids [25]. The by-products (crystalline calcium acetate) were identified through the plastic bag, as sample used in other validation techniques and confirmed the identity of the product.

Table 1. Summarized Raman bands observed in spectra of the demineralized, chitin-based foil products derived from the three crustacean species, compared to the pure α-chitin.

Chitin-based foil from *C. sapidus*	**Waste shell of *C. sapidus***	**Waste fragment of *M. squinado***	**Waste shell *S. mantis* (abdomen cuticle)**	**α-chitin Raman bands/cm^{-1}**
Hand-held TacticID Raman Instrument, 1064 nm	Renishaw InVia Reflex Raman system, 785 nm	Renishaw	Renishaw	
250,9	253		254	253
				269

 doi:10.20944/preprints202403.0918.v1

				273
325	325		325	325
				366
			369	369
	373			373
395	395			397
				429
457	456		457	458
				481
499	501		501	499
	527			530
				533
567	565			566
	599			599
658	650			649
755	709			710
899	894	898	894	899
955	953	955	952	955
				1043
1059	1059			1059
1109	1109		1108	1109
	1146		1147	1149
1266	1263	1268	1265	1266
1337	1328		1330	1328
1373	1372		1374	1378
1416	1414		1415	1415
1451	1448	1451		1451
1629	1620		1621	1622
1663	1657		1658	1657
Out of the instrument range	2880		2882	2881
	2913			2909
	2937	2937	2937	2936
	2958			2963

3.8. Morphology and Semi-Quantitative Analyses of the Demineralized Crustacean Foils Determined with SEM-EDX

SEM-EDX images show surface morphology of the treated cuticle shells at the end of the acetic acid treatment (65 days). The surface morphology of the treated *C. sapidus* fragment shows long unbroken fibers of chitin (Figure 9A left and middle image). The highest weight percentage in the fragment was for carbon and oxygen (Figure 9A right image), but there is still calcium present, probably in the form of calcium acetate. The surface morphology of the *S. mantis* (Figure 9B left and middle image) and *M. squinado* (Figure 9C left and middle image) did not reveal chitin fibers as clearly as it did for C. sapidus. The highest weight percentage in the fragments of *S. mantis* and *M. squinado*

 doi:10.20944/preprints202403.0918.v1

was for oxygen and calcium. Calcium could be resulting from calcium acetate hypertonic acetic acid bath solution, which resulted in calcium acetate crystals forming on the fragments.

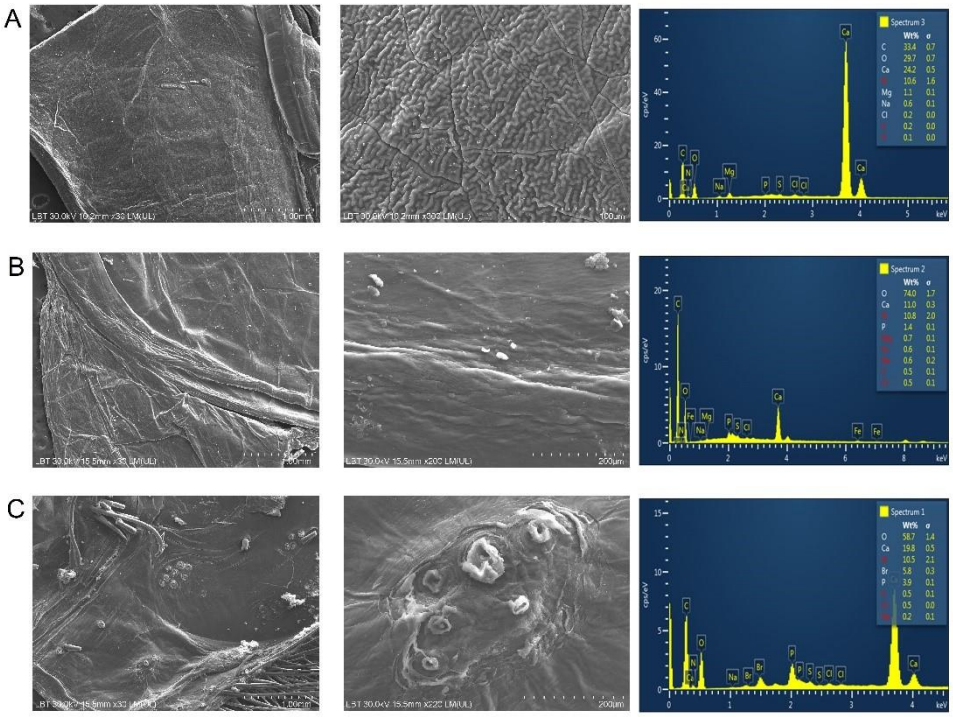

Figure 9. SEM images of the surface morphology of the acetic acid bath treated cuticle of three species with corresponding EDX graphs; *C. sapidus* (A), *S. mantis* (B) and *M. squinado* (C).

5. Conclusions

The demineralization process of the waste biogenic carbonates from crustacean and sea snail shells can be optimized and controlled by using Raman techniques and technologies. Optimization could involve monitoring the rate of waste shells demineralization in a time-dependent manner. Such process control is non-destructive and does not compromise the shells. Besides using Raman spectroscopy in laboratory settings, hand-held Raman instruments are promising and more convenient tools for monitoring the demineralization process. Moreover, obtaining chitin-based polymeric materials from the carapace or fragments of the crustacean shells, along with the recovery of calcium acetate as a by-product of interest, which can be crystalized from the treatment bath solution, exemplifies a bioeconomic process. Biogenic calcium acetate was also produced through the environmentally friendly demineralization process of *R. venosa* shells. Overall, implementing Raman techniques and technologies can be a relevant and convenient tool for successful demineralization processes, increasing the usage of reutilization of the marine waste shells for obtaining compounds of interest such as chitin and calcium acetate with various applications.

As the chitin-based polymeric materials are of increasing interest in the light of proposing a future circular carbon and plastic economy [26] centred on several targets, such as reducing and eliminating 50% of all plastic materials and products, replace all fossil-fuel-based plastics with those sourced from alternative bio-based waste, accelerating carbon recirculation through use of biomass and CO_2, minimizing environmental footprint and maximizing recycling. We expect to load such processes control tools to achieve these goals in finding technical solutions from waste to new generation polymeric materials, through the sustainable approaches to convert aquatic waste into recyclable polymers.

 doi:10.20944/preprints202403.0918.v1

Supplementary Materials: The following supporting information can be downloaded at the website of this paper posted on Preprints.org. Figure S1: Raman spectra recorded from demineralized crab shell indicating the raw data (A), their processing (averaging, background subtraction (B) and the comparison of results with the signal of α- chitin (D). Additional bands are highlighted in light yellow. (C) Raman signal of acetic acid treated shell of *C. sapidus* directly tested with a hand-held Tactic ID Raman system resembling alpha-chitin bands (red dash-lined frames). Excitation: 785 nm (A, B, D), 1064 nm (C); Video S1: Demonstration of the flexibility of the intact, transparent, demineralized foil products resulted from the three crustacean species after 65 days of acetic acid treatment.

Author Contributions: Conceptualization, S.C.P.; methodology, S.C.P., I.C.P., K. M., D.A.D.; validation, S.C.P., I.C.P., K. M., T. T., D.A.D., N. B.,; formal analysis, S.C.P., K. M., I. C. P..; investigation, S.C.P., I.C.P., K.M., D.A.D, F.N.,T.T., L.B., B.N..; resources, S.C.P, F.N., D.A.D, B.N.; data curation, S.C. P., K. M., I. P., L. B..B. N.; writing—original draft preparation,I.C.P., K.M.; writing—review and editing, S.C.P., I.C.P., K.M., D.A.D, T.T., B. N.; visualization,S.C.P., I.C.P., K.M., D.A.D., L.B-T., T.T., F. N. N. B.; supervision, S.C.P.; All authors have read and agreed to the published version of the manuscript."

Funding: This research received no external funding.

Data Availability Statement: Data supporting reported results are included in the manuscript and supplementary information.

Conflicts of Interest: The authors declare no conflicts of interest.

References

1. Bioeconomy strategy- European Comission, research-and-innovation.ec.europa.eu. Available online: Bioeconomy strategy - European Commission (europa.eu) (accessed on 2/20/2024, 9:48:16 PM)
2. Glamuzina, B., Vilizzi, L., Piria, M., Žuljević, A., Cetinić, A.B., Pešić, A., Dragičević, B., Lipej, L., Pećarević, M., Bartulović, V., Grđan, S., Cvitković, I., Dobroslavić, T., Fortič, A., Glamuzina, L., Mavrič, B., Tomanić, J., Despalatović, M., Trkov, D., Šćepanović, M.B., Vidović, Z., Simonović, P., Matić-Skoko, S., Tutman, P. Global warming scenarios for the Eastern Adriatic Sea indicate a higher risk of invasiveness of non-native marine organisms relative to current climate conditions. Mar Life Sci Technol. 2023. https://doi.org/10.1007/s42995-023-00196-9
3. Marchessaux, G., Gjoni, V., Sarà, G. Environmental drivers of size-based population structure, sexual maturity and fecundity: A study of the invasive blue crab Callinectes sapidus (Rathbun, 1896) in the Mediterranean Sea. 2023, PLoS ONE 18, e0289611. https://doi.org/10.1371/journal.pone.0289611
4. EC – Commission of the European Communities. Green paper on the management of bio-waste in the European Union. COM(2008) 811 final. URL: https://eur-lex.europa.eu/legal-content/EN/TXT/PDF/?uri=CELEX:52008DC0811&from=EN (accessed 19. Dec 2022).
5. Nekvapil, F., Pinzaru, S.C., Barbu–Tudoran, L., Suciu, M., Glamuzina, B., Tamaș, T., Chiș, V., 2020. Color-specific porosity in double pigmented natural 3d-nanoarchitectures of blue crab shell. Sci Rep 10, 2020, 3019. https://doi.org/10.1038/s41598-020-60031-4
6. Nekvapil, F., Aluas, M., Barbu-Tudoran, L., Suciu, M., Bortnic, R.-A., Glamuzina, B., Pinzaru, S.C. From Blue Bioeconomy toward Circular Economy through High-Sensitivity Analytical Research on Waste Blue Crab Shells. ACS Sustainable Chem. Eng. 7, 2019, 16820–16827. https://doi.org/10.1021/acssuschemeng.9b04362
7. Lazar, G., Nekvapil, F., Hirian, R., Glamuzina, B., Tamas, T., Barbu-Tudoran, L., Pinzaru, S.C. Novel Drug Carrier: 5-Fluorouracil Formulation in Nanoporous Biogenic Mg-calcite from Blue Crab Shells—Proof of Concept. ACS Omega 6, 2021, 27781–27790. https://doi.org/10.1021/acsomega.1c03285
8. Lazar, G., Nekvapil, F., Glamuzina, B., Tamaș, T., Barbu-Tudoran, L., Suciu, M., Cinta Pinzaru, S. pH-Dependent Behavior of Novel 5-FU Delivery System in Environmental Conditions Comparable to the Gastro-Intestinal Tract. Pharmaceutics 15, 2023, 1011. https://doi.org/10.3390/pharmaceutics15031011
9. Nekvapil, F., Mihet, M., Lazar, G., Pinzaru, S.C., Gavrilović, A., Ciorîță, A., Levei, E., Tamaș, T., Soran, M.-L., Comparative Analysis of Composition and Porosity of the Biogenic Powder Obtained from Wasted Crustacean Exoskeletonsafter Carotenoids Extraction for the Blue Bioeconomy. Water 15, 2023, 2591. https://doi.org/10.3390/w15142591
10. Nekvapil, F., Ganea, I.-V., Ciorîță, A., Hirian, R., Tomšić, S., Martonos, I.M., Cintă Pinzaru, S. A New Biofertilizer Formulation with Enriched Nutrients Content from Wasted Algal Biomass Extracts Incorporated in Biogenic Powders. Sustainability 13, 2021, 8777. https://doi.org/10.3390/su13168777
11. Nekvapil, F., Ganea, I.-V., Ciorîță, A., Hirian, R., Ogresta, L., Glamuzina, B., Roba, C., Cintă Pinzaru, S. Wasted Biomaterials from Crustaceans as a Compliant Natural Product Regarding Microbiological,

 doi:10.20944/preprints202403.0918.v1

Antibacterial Properties and Heavy Metal Content for Reuse in Blue Bioeconomy: A Preliminary Study. Materials 14, 2021, 4558. https://doi.org/10.3390/ma14164558

12. Younes, I., Rinaudo, M. Chitin and Chitosan Preparation from Marine Sources. Structure, Properties and Applications. Marine Drugs 13, 2015, 1133–1174. https://doi.org/10.3390/md13031133
13. Gadgey, K. K., Bahekar, A. Studies on extraction methods of chitin from crab shell and investigation of its mechanical properties. IJMET 8:2, 2017, 220–231. https://www.academia.edu/57937995/Study_on_Chitin_Extraction_from_Crab_Shells_Waste
14. Gortari, M.C., Hours, R.A. Biotechnological processes for chitin recovery out of crustacean waste: A mini-review. Electron. J. Biotechnol. 16, 2013 https://doi.org/10.2225/vol16-issue3-fulltext-10
15. GRAS Notice (GRN) No. 712 https://www.fda.gov/Food/IngredientsPackagingLabeling/GRAS/NoticeInventory/default.htm
16. Iftekhar Shams, Md., Nogi, M., Berglund, L.A., Yano, H., 2012. The transparent crab: preparation and nanostructural implications for bioinspired optically transparent nanocomposites. Soft Matter 8, 2012, 1369–1373. https://doi.org/10.1039/C1SM06785K
17. Metrohm, available online: https://www.metrohm.com/ro_ro/products/b/wt-8/bwt-840000920.html (accessed 02/21/2024, 11:5)
18. Watling, L., Thiel, M. (Eds.), 2013. The natural history of the Crustacea. Oxford University Press, Oxford; New York, 2013, 141-148
19. Dahmane, E.M., Taourirte, M., Eladlani, N., Rhazi, M. Extraction and Characterization of Chitin and Chitosan from *Parapenaeus longirostris* from Moroccan Local Sources. International Journal of Polymer Analysis and Characterization 19, 2014, 342–351. https://doi.org/10.1080/1023666X.2014.902577
20. Vino, A.B., Ramasamy, P., Shanmugam, V., Shanmugam, A. Extraction, characterization and in vitro antioxidative potential of chitosan and sulfated chitosan from Cuttlebone of Sepia aculeata Orbigny, 1848. Asian Pacific Journal of Tropical Biomedicine 2, 2012, S334–S341. https://doi.org/10.1016/S2221-1691(12)60184-1
21. Kaya, M., Sargin, I., Aylanc, V., Tomruk, M.N., Gevrek, S., Karatoprak, I., Colak, N., Sak, Y.G., Bulut, E. Comparison of bovine serum albumin adsorption capacities of α-chitin isolated from an insect and β-chitin from cuttlebone. Journal of Industrial and Engineering Chemistry 38, 2016, 146–156. https://doi.org/10.1016/j.jiec.2016.04.015
22. Musumeci, A.W., Frost, R.L., Waclawik, E.R. A spectroscopic study of the mineral paceite (calcium acetate). Spectrochimica Acta Part A: Molecular and Biomolecular Spectroscopy 67, 2007, 649–661. https://doi.org/10.1016/j.saa.2006.07.045
23. Miller, J.R., LaLama, M.J., Kusnic, R.L., Wilson, D.E., Kiraly, P.M., Dickson, S.W., Zeller, M. On the nature of calcium magnesium acetate road deicer. Journal of Solid State Chemistry 270, 2019, 1–10. https://doi.org/10.1016/j.jssc.2018.10.041
24. Koleva, V. Vibrational Behavior of Calcium Hydrogen Triacetate Monohydrate, $CaH(CH_3COO)_3H2O$, CROATICA CHEMICA ACTA, 78 (4), 2005, 581-591
25. Khoushab, F., Yamabhai, M. Chitin Research Revisited. Marine Drugs 8, 2010, 1988–2012. https://doi.org/10.3390/md8071988
26. Vidal, F., Van Der Marel, E.R., Kerr, R.W.F., McElroy, C., Schroeder, N., Mitchell, C., Rosetto, G., Chen, T.T.D., Bailey, R.M., Hepburn, C., Redgwell, C., Williams, C.K. Designing a circular carbon and plastics economy for a sustainable future. Nature 626, 2024, 45–57. https://doi.org/10.1038/s41586-023-06939-z